Advances in Redox Research 1 (2021) 100001

Contents lists available at ScienceDirect

Advances in Redox Research

journal homepage: www.elsevier.com/locate/arres

The influence of dibenzocyclooctadiene lignans on macrophage glutathione and lipid metabolism associated with *Chlamydia pneumoniae*-induced foam cell formation

Maarit Kortesoja, Eveliina Taavitsainen, Leena Hanski*

Drug Research Program, Division of Pharmaceutical Biosciences, Faculty of Pharmacy, University of Helsinki, P.O. Box 56 (Viikinkaari 5E), FI-00014 University of Helsinki, Helsinki, Finland

ARTICLE INFO

Keywords:
Schisandra chinensis
Oxidative stress
Oxidized low-density lipoprotein
Atherosclerosis
Antichlamydial agent

ABSTRACT

Triggered by changes in macrophage redox status and lipid metabolism, foam cells represent a hallmark of atherosclerosis. Induction of macrophage foam cell formation by *Chlamydia pneumoniae*, a gram-negative human pathogen, has been established in various earlier studies *in vitro* and *in vivo*. Oxidation of low-density lipoprotein (LDL) by *C. pneumoniae* and alterations in macrophage lipid metabolism do not require chlamydial replication, making conventional antibiotics useless in the intervention of the process. In this work, we report on the ability of schisandrin B and schisandrin C, two dibenzocyclooctadiene lignans, to suppress the *C. pneumoniae* -induced foam cell formation in RAW264.7 macrophages. This effect was accompanied with the upregulation of *PPARγ*, a nuclear receptor acting as a major transcriptional regulator of lipid metabolism and inflammatory responses. Schisandrin B and schisandrin C also increased the total intracellular glutathione content of the macrophages. In the case of schisandrin B, this was accompanied with the upregulation of GSH biosynthetic genes glutamate cysteine ligase (both the catalytic and the modifier subunits *GCLc* and *GCLm*) as well as gamma-glutamyl transpeptidase *GGT1*. In addition, schisandrin B and schisandrin C upregulated the expression of a lipid transport protein *ABCA1* gene mediating cholesterol efflux from macrophages translating into a reduction in total cholesterol concentration in the schisandrin B -treated cells. Collectively, these data indicate that both schisandrin B and schisandrin C are able to alleviate the pathogenic consequences of *C. pneumoniae* infection in macrophages by altering the cellular redox balance and lipid trafficking.

Introduction

Cardiovascular diseases (CVD), including stroke and myocardial infarction, are the leading causes of death in the world [1]. The main underlying factor of most CVD is atherosclerosis which is a chronic inflammatory condition involving interaction between monocyte derived macrophages, T cells, arterial walls and modified lipoproteins [2]. The initial triggers of atherosclerosis are the oxidation of low-density lipoproteins (LDL) and accumulation of inflammatory cells to arterial wall. In atherosclerotic lesions the immune cells secrete cytokines and thus promote the proinflammatory environment [3]. Eventually, cellular lipids accumulate into macrophages as lipid vacuoles and the cells are converted into foam cells which is considered one of the hallmarks of early atherosclerosis [4].

Monocyte derived macrophages play a central role in cholesterol metabolism [5]. Under proinflammatory and oxidative conditions, the uptake of oxidized LDL (oxLDL) into these cells is increased while cholesterol efflux is reduced, leading to the accumulation of esterified cholesterol into the lipid droplets in the cytoplasm. Thus, oxidative stress is one of the key underlying factors in atherosclerosis [6]. The macrophage foam cell formation during early atherogenesis is determined by the oxidative state and antioxidant levels in these cells, because they translate to the degree of LDL oxidation.

Abbreviations: ACAT1, acyl coenzyme A cholesterol acyltransferase 1; AP-1, activator protein 1; BSO, buthionine sulfoximine; CVD, cardiovascular diseases; CD-36, cluster of differentiation 36; DTNB, 5.5-dithio-bis(2-nitrobenzoic acid); GCL, glutamate cysteine ligase; GGT, γ-glutamyl transpeptidase; GSH, glutathione; IL, interleukin; JNK, c-Jun N-terminal kinase; LDL, low-density lipoprotein; MAPK, mitogen-activated protein kinase; MOI, multiplicity of infection; NADPH, nicotinamide adenine dinucleotide phosphate; NF- κB, nuclear factor- κB; NOD, nucleotide-binding oligomerization domain-containing protein; PBMN, peripheral blood mononuclear cells; PPARγ, peroxisome proliferator-activated receptor γ; ROS, reactive oxygen species; SR-A, scavenger receptor A; TLR, Toll like receptor; TNF-α, tumor necrosis factor α; γGC, γ-glutamylcysteine.

* Corresponding author.
E-mail address: leena.hanski@helsinki.fi (L. Hanski).

https://doi.org/10.1016/j.arres.2021.100001
Received 18 December 2020; Received in revised form 8 February 2021; Accepted 9 February 2021
Available online 13 February 2021

Glutathione (GSH) is a major small-molecule antioxidant in the cells and disruptions in glutathione metabolism are associated with atherosclerosis development [7,8]. Decreased GSH levels enable the accumulation of excess reactive oxygen species (ROS) which promotes the generation of oxidatively modified molecules such as oxLDL. In addition, ROS initiate redox signaling cascades, leading to e.g. nuclear factor κB (NF-κB) and activator protein 1 (AP-1) activation [9].

The biosynthesis of GSH inside mammalian cells involves two enzymatic reactions [10]. First glutamate cysteine ligase (GCL) produces γ-glutamylcysteine (γGC) from glutamic acid and cysteine. Glutathione synthase then catalyzes the GSH formation from γGC and glycine. Once generated, the oxidized form of glutathione can be transported from cytosol to extracellular space to maintain cellular and systemic redox status [11]. In the extracellular space, glutathione is broken down by γ-glutamyl transpeptidase (GGT). By breaking down extracellular GSH and providing components for *de novo* synthesis of GSH, including the rate limiting amino acid cysteine, GGT activity is involved in the synthesis of GSH.

In macrophages, scavenger receptors CD36, scavenger receptor A (SR-A) and lectin-like oxidized low-density lipoprotein receptor-1 (LOX-1) are mostly responsible for the oxLDL uptake [5]. Among them, CD36 prefers mildly oxidized forms of LDL and mediates the activation of c-Jun N-terminal kinase (JNK) signaling which has a central role in foam cell formation [12,13]. On the other hand, cholesterol export occurs via pathway known as reverse cholesterol transport (RCT) [14]. Lipid accumulation in macrophages induces the efflux of cholesterol, mainly occurring via ABC transporters ABCA1 and ABCG1 [15].

In addition to oxLDL internalization and cholesterol export, the esterification of cholesterol is also one of the key factors involved in the macrophage lipid metabolism [16]. Once lipoproteins are taken into the cells free cholesterol is esterified by acyl coenzyme A cholesterol acyltransferase 1 (ACAT1). Esterified cholesterol is more likely taken into lipid droplets and promotes the lipid accumulation [17].

One major regulator of the macrophage lipid metabolism is the nuclear receptor peroxisome proliferator-activated receptor γ (PPARγ). Oxidized fatty acid internalized by CD36 act as high-affinity ligands for PPARγ, leading to transcriptional regulation of PPARγ target genes. This yields a proatherogenic regulatory loop by the induction of *CD36* transcription [18] and *ACAT1* transcription [4]. On the other hand, PPARγ activation also results in the upregulation of *ABCA1* and *ABCG1* genes, enhancing lipid efflux in macrophages [19,20].

A central pathogenic mechanism of atherosclerosis is chronic inflammation [21]. Infectious burden is considered a risk factor for atherosclerosis and the involvement of chronic infections has been suggested in the development of the disease [22]. One of the most widely studied pathogens in this context is *Chlamydia pneumoniae* [21,23]. *C. pneumoniae* is a gram-negative, obligate intracellular bacterium that primarily infects respiratory tract [24]. It disseminates from lung epithelium to other body sites via peripheral blood mononuclear cells (PBMN), monocytes and macrophages [25,26]. Viable and cultivable forms of *C. pneumoniae* have been isolated from atherosclerotic arterial walls, but not from healthy arteries [27–29]. In addition, several animal models endorse the role of *C. pneumoniae* in the onset and progression of chronic inflammatory diseases [30–32]. *C. pneumoniae* is also reported to turn spontaneously into persistent form in PBMCs [33–35].

Upon the persistent infection, *C. pneumoniae* has been shown to alter the normal functions of macrophages in several ways; it induces foam cell formation [36], alters cytokine production, changes monocyte maturation process and enhances adhesion and migration [25]. While chlamydial lipopolysaccharide (cLPS) is able to trigger macrophage foam cell formation [36], *C. pneumoniae* heat shock protein 60 (hsp60) contributes to the process by promoting the oxidation of LDL [37,38]. Heat and UV-inactivated *C. pneumoniae* disturb the cholesterol homeostasis in macrophages in a fashion similar to viable bacteria [39], which further supports the view that chlamydial replication is not needed to trigger the macrophage foam cell formation.

According to earlier studies, the interconnected actions of mitogen-activated protein kinase (MAPK) and PPARγ signaling have a central role in the *C. pneumoniae* -induced foam cell formation [40]. JNK signaling is the most prominent MAPK pathway in this respect [41] which is also demonstrated by the inhibitory role of the JNK1/2 inhibitor SP600125 on *C. pneumoniae*-induced foam cell formation [42]. In addition, *C. pneumoniae* infection inhibits ABCA1 expression and cholesterol efflux in mice [21].

As bacterial replication is not required for *C. pneumoniae* -induced macrophage lipid accumulation, traditional antibiotics do not prevent or suppress *C. pneumoniae* -induced foam cell formation. Our previous studies revealed the antichlamydial activity of dibenzocyclooctadiene lignans originating from a medicinal plant *Schisandra chinensis* [43]. We have also shown that treatment with these lignans has a chemosensitizing effect on the persistent *C. pneumoniae* infection in THP-1 macrophages, by significantly improving the bacterial eradication by a standard of care antibiotic azithromycin [33].

Given the previous reports on the ability of *S. chinensis* lignans to alter cellular redox balance and the well-established role of oxidative stress in macrophage foam cell formation, it was of interest to examine the effect of the dibenzocyclooctadiene lignans on *C. pneumoniae* -induced foam cell formation as well as on lipid and glutathione metabolism in macrophages. The impact of schisandrin, schisandrin B and schisandrin C on foam cell formation, intracellular glutathione and cholesterol levels as well as their impact on the expression of genes involved in glutathione and cholesterol metabolism were studied in murine RAW264.7 macrophages.

Materials and methods

Compounds

Schisandrin was purchased from Sigma-Aldrich (St. Louis, MO, USA) and schisandrin B and schisandrin C were from Fine Tech Industries (London, UK) (Fig. 1). Compounds were diluted in concentration of 20 mM in DMSO. Buthionine sulfoximine (BSO) was purchased from Sigma-Aldrich (St. Louis, MO, USA) and it was diluted as 100 mM concentration in H_2O. JNK1/2 inhibitor SP600125 was purchased from Tocris Bioscience (Bristol, UK) and diluted in DMSO in concentration of 20 mM.

Cell culture

Murine macrophage cell line RAW264.7 (ATCC TIB-71) were purchased from American Type Culture Collection (ATCC). The cells were grown in Dulbecco's Modified Eagle Medium (DMEM) (Gibco, Invitrogen, Thermo Fisher Scientific, Paisley, UK) with 10% Fetal bovine serum (FBS) (BioWhittaker, Lonza, Basel, Switzerland) and 20 μg/ml Gentamicin (Fluka, Buchs, Switzerland) and maintained in 37°C, 5% CO_2 and 95% humidity in 75 cm^2 cell culture flasks and subcultured when reached confluence. Cells were seeded into 6- or 24-well plates one day prior to experiments at densities indicated below.

Cell viability assay

The impact of schisandrin, schisandrin B, schisandrin C and BSO on RAW264.7 cell viability were studied with resazurin cell viability assay. The cells were seeded into 24-well plates at a density at 1×10^5 cells/ml. The lignans were added at 25 μM and 50 μM concentration, and positive control, usnic acid at 10 μM concentration, and the cultures were incubated for 24 or 48 h. Resazurin (Sigma-Aldrich, 3 mM stock dissolved in H2O) was added to yield a final concentration of 20 μM. Cells were incubated for 2 h, 200 μl of the culture medium from each well was transferred into a 96-well plate and fluorescence was recorded at 570/590 nm with Varioskan Lux plate reader (Thermo Fisher scientific).

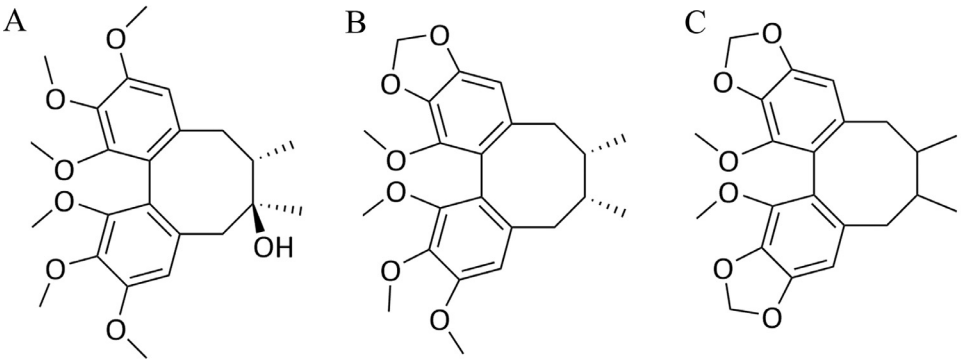

Fig. 1. Chemical sructures of (A) schisandrin (B) schisandrin B and (C) schisandrin C. All three lignans contain the core dibenzocyclooctadiene structure and they only differ by side chains. Schisandrin differs from the others by having hydroxyl group bound in the cyclooctadiene ring. In addition, schisandrin B contains one and schisandrin C two methylenedioxy groups which replace two corresponding free hydroxyl groups present in the schisandrin structure.

C. pneumoniae *infection*

C. pneumoniae clinical isolate, CV6, from an atherosclerotic artery [44] was obtained from professor Matthias Maass (Paracelsus Medical University, Salzburg, Austria) and propagated in HL cells [45] as previously described [46]. Cells were infected with multiplicity of infection (MOI) 1 or MOI 5. The *C. pneumoniae* inoculum was added on the cell monolayer in 6- or 24-well plate, centrifuged at 550 *g* for 1h, and incubated at 37°C for another hour. Then inoculum was removed and 1 ml culture medium with the studied compounds were added to the wells, followed by an incubation for 24 or 48 h.

Foam cell formation assay

RAW264.7 cells were seeded into 24-well plates at a density at 1×10^5 cells/ml and infected with MOI 1 of *C. pneumoniae*. Cells were incubated with 50 μM schisandrin lignans, 250 μM BSO or 10 μM SP600125 and 25 μg/ml of LDL (Sigma-Aldrich) for 48 h. The studied compounds and LDL were added to the cells at the same time, after removing the bacterial inoculum from the wells. After the 48 h incubation cells were washed two times with PBS and fixed with 4% paraformaldehyde (PFA, Santa Cruz Biotechnology, Dallas, TX, USA) for 15 min. Then, cells were washed 2 times with H_2O and incubated 5 min with 1 ml 60% isopropanol. After that, cells were dried in RT and 5 mM Oil Red O (Sigma- Aldrich) solution was added to the wells and incubated for 10 min. The staining solution was removed, and cells were washed 4 times with H_2O. Water was left to the wells and the cells were analyzed under EVOS Cell Imaging System (Thermo Fisher scientific) using the 20 × magnification.

Glutathione quantitation

The intracellular total glutathione levels of RAW264.7 macrophages were determined using an enzymatic recycling method described previously by Rahman et al [47]. In brief, cells were seeded into 6-well plates at a density of 2×10^5 cells/ml and the monolayer was incubated with schisandrin lignans or BSO for 24 or 48 h. Then, cells were collected, washed with PBS and resuspended into extraction buffer and lysed. Glutathione concentrations were determined based on its reaction with 5.5-dithio-bis(2-nitrobenzoic acid) (DTNB) in the presence of glutathione reductase (GR) and β-nicotinamide adenine dinucleotide phosphate (β-NADPH). Formation of TNB was measured with Multiskan sky plate reader set to 412 nm. Also GSSG levels were assayed but they remained below the detection limit of the assay and are thus not reported.

For data normalization, total protein concentration determination of the cell lysates was performed with acetone precipitation. 100 μl of cell lysate sample was heated 5 min at 95°C and 400 μl of cold (-20°C) acetone was added. The sample was mixed and incubated 1 h at -20°C, centrifuged at 15000 *g* and the supernatant was discarded. The pellet was resuspended to 100 mM Tris-buffer (pH; 7.5) and protein concentration was detected with Multiskan sky, μDrop plate (Thermo Fisher Scientific).

Total cholesterol and cholesteryl ester quantification

RAW264.7 macrophages were seeded into 24-well plates at a density at 1×10^5 cells/ml. Cells were infected with *C. pneumoniae* at MOI 5. Schisandrin, schisandrin B, schisandrin C (50 μM) and BSO (250 μM) in the presence of 25 μg/ml LDL (Sigma-Aldrich) were added to the wells and the cultures were incubated for 48 h.

The levels of total cholesterol and cholesteryl esters were determined from the macrophages with Amplex© Red cholesterol assay kit (Invitrogen) by modifying manufacturer's instructions. In brief, the cells were fixed with 2% PFA and washed 3 times with PBS. The lipids were extracted with ethanol, 200 μl/well, by incubating 30 min at 4°C. The sample was prepared by mixing 40 μl of ethanol-lipid solution and 60 μl of reaction buffer. For determining the concentration of total cholesterol 50 μl of sample was incubated with 50 μl of assay solution (150 μM Amplex© Red solution, 1 U/ml HRP, 1 U/ml cholesterol oxidase, 0.1 μM cholesterol esterase and reaction buffer). For the free cholesterol quantification, the sample was incubated with a similar assay solution but without cholesterol esterase. Both solutions were incubated 30 min at 37°C, protected from light and the fluorescence was recorded with Varioskan Lux plate reader set to 540/590 nm. The cholesterol concentrations (μg/ml) were determined from a six-point standard curve. The fraction of esterified cholesterol was calculated based on the concentrations of the free and the total cholesterol.

Quantitative reverse transcription PCR

RAW264.7 cells were seeded into 24-well plates at a density of 1×10^5 cells/ml. Cells were either infected or not infected with *C. pneumoniae*, MOI 5, as described above, and treated with 50 μM schisandrin, schisandrin B and schisandrin C. 250 μM BSO was used as a control. Cells were incubated for 48 h and after that cells were lysed and RNA was isolated with PureLink RNA Mini Kit (Ambion, life technologies, Thermo Fisher Scientific) according to the manufacturer's instructions. The RNA was then used as a template for cDNA synthesis, which was performed with RevertAid First Strand cDNA Synthesis Kit (Thermo Fisher Scientific). The reactions were carried out in 20 μl volumes including template RNA, Oligo $(dT)_{18}$ primers, nucleotides and revertAid reverse transcriptase. The cDNA concentrations were determined with NanoDrop (Thermo Fisher Scientific) and the expression of studied genes were examined with Step One Plus Real-Time PCR system (Thermo Fisher Scientific), using, GAPDH as a reference housekeeping gene. The primers used for each of the studied genes are listed in Table 2.

Data analysis

The SPSS Statistics 25 software was used for statistical analysis. Statistical significances of the GSH level analysis and cholesterol level anal-

Table 1
Host cell viability after treatment with studied compounds.

Compound	Viability-%
Schisandrin 25 μM	97.9 ± 0.9
Schisandrin 50 μM	99.0 ± 2.2
Schisandrin B 25 μM	86.7 ± 0.8
Schisandrin B 50 μM	61.0 ± 3.2
Schisandrin C 25 μM	102.6 ± 2.9
Schisandrin C 50 μM	101.4 ± 1.6
BSO 250 μM	113.0 ± 1.2
Usnic acid 10 μM	13.5 ± 0.05

Viability data are normalized to the values of 0.25% DMSO control.

Table 2
Primers used in the RT-PCR analysis.

Gene	Primers
PPAR-γ	Forward: 5'- GAC ATC CAA GAC AAC CTG CTG -3'
	Reverse: 5'- GCA ATC AAT AGA AGG AAC ACG -3'
CD36	Forward: 5'- TCG GAA CTG TGG GCT CAT TG -3'
	Reverse: 5'- CCT CGG GGT CCT GAG TTA TAT TTT C -3'
ABCA1	Forward: 5'- CAA CTA CAA AGC CCT CTT TG -3'
	Reverse: 5'- CTT GGC TGT TCT CCA TGA AG -3'
ACAT1	Forward: 5'- TTT ATT GCA AGG CGC TCT CT -3'
	Reverse: 5'- GAA CTC AAG CAC CAG CCT TC -3'
GCLc	Forward: 5'- ATG TGG ACA CCC GAT GCA GTA TT -3'
	Reverse: 5'- TGT CTT GCT TGT AGT CAG GAT GGT TT -3'
GCLm	Forward: 5'- GCC ACC AGA TTT GAC TGC CTT T -3'
	Reverse: 5'- CAG GGA TGC TTT CTT GAA GAG CTT -3'
GGT1	Forward: 5'- GGA GAG AGT TTC TGC CCA TCC ATA C -3'
	Reverse: 5'- GCG GCT GGG TGG GTG GT -3'

ysis were determined by One-way ANOVA and Dunnett's T post hoc test, and data are shown as mean ± SEM. In gene expression analysis, the expression level of each gene was compared to GAPDH expression and the results were obtained using the 2^-ΔΔCt analysis. Statistical significances of the gene expression analysis were determined by Student's T-test or One-way ANOVA and Dunnett's T post hoc test, using ΔCt values. A minimum of three biological replicates were used throughout the studies.

Results

Impact of schisandrin lignans on host cell viability

The host cell viability was studied with resazurin assay. Cells were treated with 25 μM and 50 μM of schisandrin lignans and 250 μM of BSO for 24 h. The 10 μM of usnic acid was used as positive control. Usnic acid was toxic to the cells and the cell viability was only 13%. Neither of schisandrin lignans reduced the viability statistically significantly as shown in Table 1.

Impact of schisandrin lignans on C. pneumoniae *induced foam cell formation*

The *C. pneumoniae* induced foam cell formation in RAW264.7 macrophages were studied by staining the lipid droplets in the cells using Oil Red O staining. The effect of 50 μM schisandrin lignans, 250 μM BSO and 10 μM SP600125, a JNK1/2 inhibitor on lipid accumulation, in presence of 25 μg/ml of LDL, were examined. Consistent with earlier reports, *C. pneumoniae* infection clearly increased the lipid accumulation in the cells inducing a foam cell -like appearance (Fig. 2A and B). Schisandrin had no effect (Fig. 2E) but schisandrin B (Fig. 2F), schisandrin C (Fig. 2G) and SP600125 (Fig. 2D) eliminated lipid accumulation effectively after 48 h treatment. The glutathione synthesis inhibitor BSO increased the foam cell formation even more pronouncedly than *C. pneumoniae* infection (Fig. 2C), which is in line with previous findings on the role of glutathione homeostasis in foam cell formation [7].

Impact of schisandrin lignans on glutathione levels in RAW264.7 macrophages

The cellular glutathione content controls the local oxidative environment and among other things, affects macrophage foam cell formation [7]. Since previous work on the schisandrin lignans indicate their ability to affect cellular glutathione metabolism in a context-dependent manner, we measured the GSH levels of RAW264.7 macrophages after 24 and 48 h exposure to 25 and 50 μM schisandrin lignans. The glutathione synthesis inhibitor BSO (250 μM) was used as a control.

According to these data, schisandrin did not affect the RAW264.7 glutathione levels at either concentrations or incubation times (Fig. 3). On the contrary, schisandrin C increased the GSH levels after 48 h with both 25 μM (76.3%, $p = 0.02$) and 50 μM (110.1%, $p = 0.0005$) concentration. Schisandrin B seemed to also increase the glutathione levels after 48 h with 25 μM (48.6%, $p = 0.23$) and 50 μM (59.8 %, $p = 0.093$), but the changes did not reach statistical significance. Similar results were also obtained when quantifying cellular GSH levels upon the concomitant *C. pneumoniae* infection and lignan treatment. Also in this case, schisandrin C yielded significant elevation of RAW264.7 GSH pools ($p = 0.007$) while the impact of schisandrin B treatment did not reach statistical significance compared to an infection control.

The impact of schisandrin lignans on total cholesterol and cholesteryl ester levels in RAW264.7 macrophages

Next, the total cholesterol and cholesteryl ester levels of RAW264.7 cells were determined with Amplex© red reagent. Cells were infected with MOI 5 of *C. pneumoniae*, exposed to 50 μM schisandrin, schisandrin B, schisandrin C and 250 μM BSO for 48 h, in the presence of 25 μg/ml of LDL.

According to these data, BSO had a significant impact on total cholesterol levels, compared to infection control, by elevating the levels by 19.4% ($p = 0.004$) (Fig. 4). Schisandrin B -treatment reduced the total cholesterol levels by 18.9% ($p = 0.005$). The cholesteryl ester levels were calculated by reducing the free cholesterol from total cholesterol levels. Both schisandrin B and schisandrin C showed tendency to suppress the degree of cholesterol esterification yet the changes did not reach statistical significance.

The impact of schisandrin lignans on expression of genes involved in lipid and GSH metabolism

The RT-PCR analysis were performed to compare the expressions of genes taking part in lipid and GSH metabolism, between the *C. pneumoniae* infected samples and between schisandrin lignan treated and untreated samples. The expression of *PPARγ, CD36, ABCA1, ACAT1, GCLc, GCLm* and *GGT1* were detected and compared to the expression of an internal reference gene *GAPDH*. To evaluate the impact of *C. pneumoniae* infection on gene expression RAW264.7 cells were infected with MOI 5 and incubated for 48 h in the presence or absence of LDL. In the samples lacking LDL, there were no statistically significant differences in the gene expression between the infected and uninfected samples (data not shown). When the cells were infected and concomitantly treated with 25 μg/ml LDL the expression of *PPARγ* and *ACAT1* was downregulated compared to the uninfected but LDL-treated controls (RQ 0.4, $p = 0.045$ and 0.4, $p = 0.1$, respectively) (Table 3). For the rest of the studied genes, no changes in expression were observed between infected and noninfected samples.

Next, cells were treated with 50 μM concentrations of schisandrin lignans for 48 h. The impact of the lignan treatment on gene expression were determined, as well as expression levels after concomitant exposure of the cells to *C. pneumoniae* infection and lignan treatment. As pre-

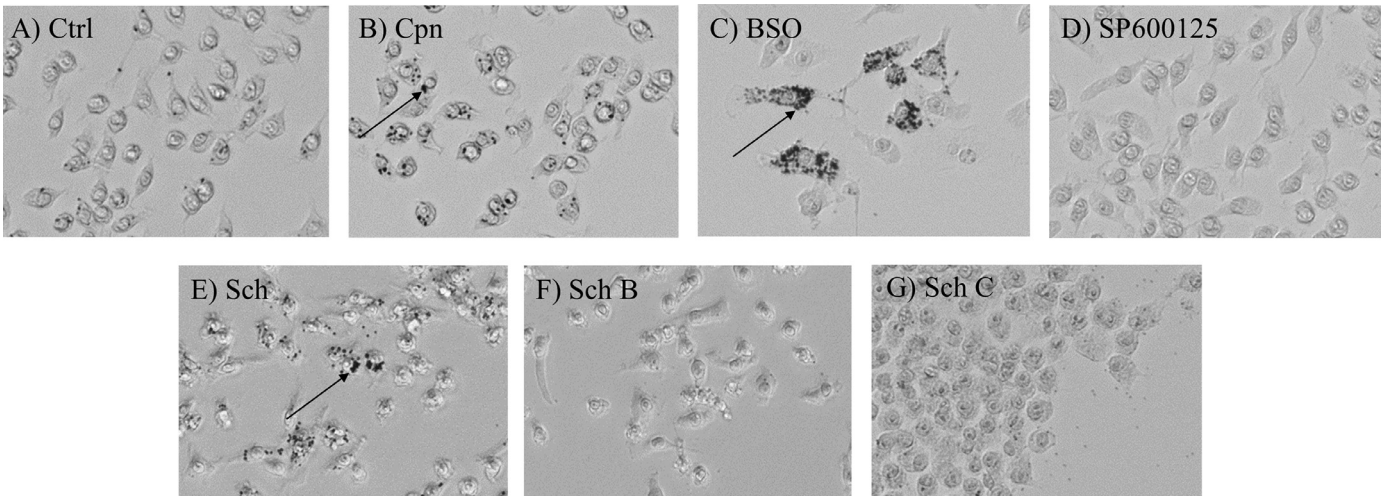

Fig. 2. The impact of schisandrin lignans on foam cell formation in RAW264.7 macrophages. Cells were infected with *C. pneumoniae* (MOI 1) and incubated with schisandrin lignans, BSO or JNK1/2 inhibitor SP600125 for 48 h in presence of LDL. Cells were stained with Oil Red O and analyzed under microscope and compared to non-infected control. Black arrows indicate the lipid droplets inside the cells. (A) Non-infected control, (B) vehicle-treated Infection, (C) treatment with 250 μM BSO, (D) treatment with 10 μM SP600125, (E) treatment with 50 μM Schisandrin, (F) treatment with 50 μM Schisandrin B, (G) treatment with 50 μM Schisandrin C. All samples include 25 μg/ml LDL.

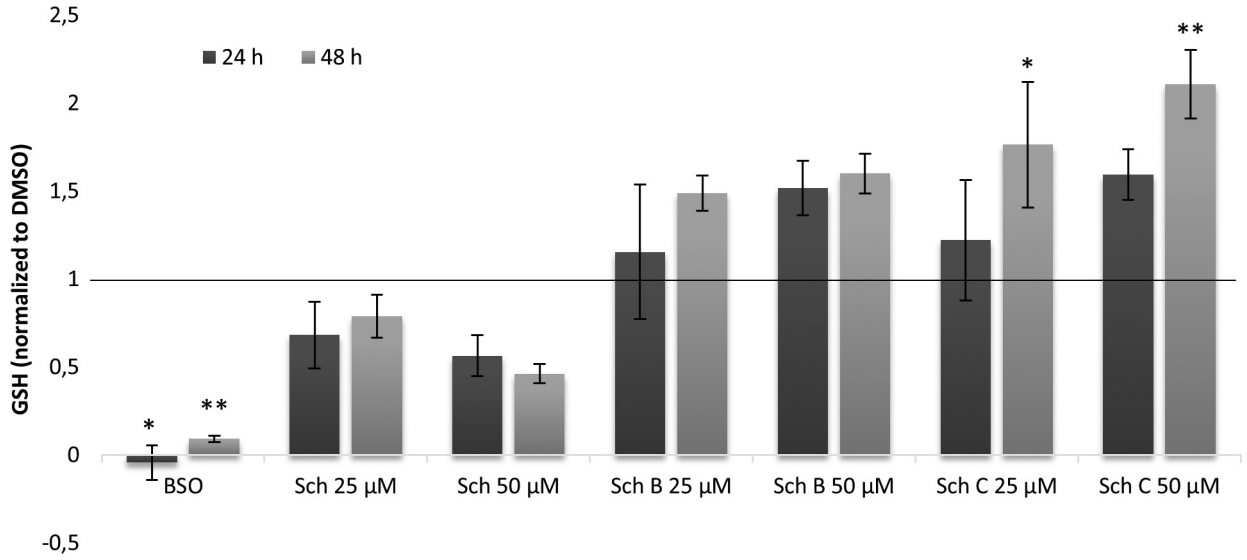

Fig. 3. The impact of schisandrin lignans on total cellular glutathione levels in RAW264.7 macrophages. Cells were incubated with schisandrin lignans for 24 and 48 h and glutathione levels were determined by using the enzymatic recycling method with DTNB and compared to vehicle control. Glutathione concentrations are normalized to the total protein content of each sample. Data are presented as mean ± SEM. Statistical significances are determined using one-way ANOVA and Dunnett's T post hoc test and they are presented as marks of *p*-values: < 0.05: *; < 0.01: **; < 0.001: ***, $n = 4$.

sented in Table 4, schisandrin B and schisandrin C increased the *PPARγ* expression in both infected and noninfected cells. In infected samples, the increase in *PPARγ* expression by schisandrin B and schisandrin C treatment was accompanied with the increased expression of the scavenger receptor *CD36*, which is known to be transcriptionally regulated by PPARγ [18]. Also *ACAT1*, another lipid metabolism mediator under PPARγ transcriptional control, showed increased expression upon the lignan treatment.

Interestingly, the three lignans showed differential effects on the *ABCA1* cholesterol efflux protein gene expression. While schisandrin decreased the *ABCA1* expression in both infected and noninfected cells, schisandrin B and schisandrin C treatment caused a significant upregulation in the *ABCA1* gene.

Regarding the genes involved in glutathione biosynthesis, schisandrin B was found to increase the expression of both the catalytic and modifier subunits of glutamate cysteine ligase (*GCLc* and *GCLm*) as well as *GGT-1*, a key enzyme in the γ-glutamyl cycle controlling the intracellular availability of GCL substrates. A statistically significant increase in the *GCL* modifier subunit (*GCLm*) was observed also in schisandrin C treated samples, while *GCLc* and *GGT-1* expression levels were not significantly affected. Schisandrin also seemed to increase the *GGT-1* expression, but not reach statistical significance.

Discussion

The phylogenetically distinct chlamydial pathogens exhibit various unique features among gram-negative bacteria. Induction of macrophage foam cell formation by *C. pneumoniae* has been established in several earlier studies *in vitro* and *in vivo* [48,49]. One fundamental underlying factor of this phenomenon is that *C. pneumoniae* triggers the

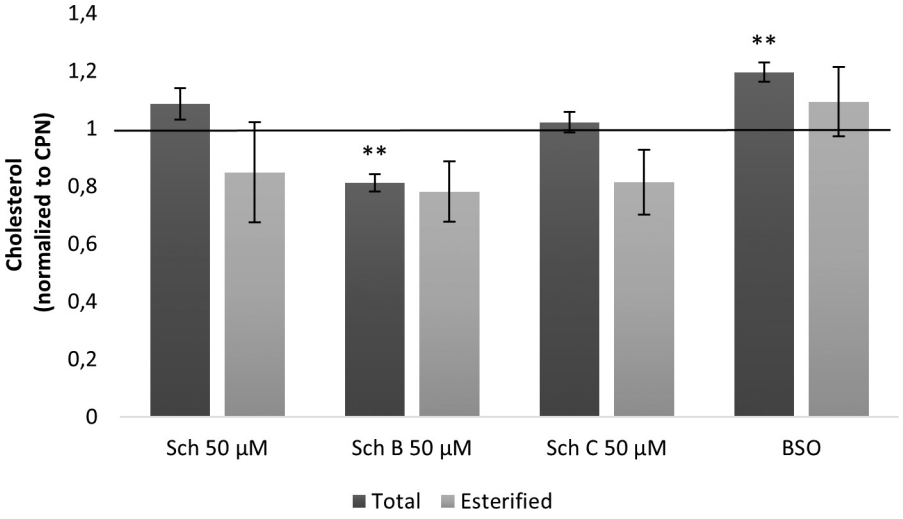

Fig. 4. The impact of schisandrin lignans on total cholesterol and cholesteryl ester levels in *C. pneumoniae* -infected RAW264.7 macrophages. Cells were infected as described under Materials and methods and incubated with the schisandrin lignans for 48 h in the presence of 25 µg/ml LDL. Cholesterol levels were determined with Amplex© Red reagent and compared to the infection control. Data are presented as mean ± SEM. Statistical significances are determined using one-way ANOVA and Dunnett's T post hoc test and they are presented as marks of *p*-values: < 0.05: *; < 0.01: **; < 0.001: ***, $n = 6$.

Table 3
The impact of *C. pneumoniae* infection on the expression of genes involved in lipid and glutathione metabolism.

Gene	Effect on expression	RQ value
PPARγ	decreasing	0.4 ± 0.08* (*p*=0.045)
CD36	-	0.9 ± 0.04
ABCA1	-	1.8 ± 0.4
ACAT1	decreasing	0.4 ± 0.1
GCLc	-	0.8 ± 0.06
GCLm	-	0.9 ± 0.09
GGT1	-	0.6 ± 0.05

The amplification of each gene was compared to an internal reference gene GAPDH and the results were obtained by using the 2^-ΔΔCt analysis. Fold changes of RQ values above 2 and below 0.5 are considered as significant and presented as bold. Statistical significances were applied from ΔCt values, using Students *t*-test and they are presented as marks of *p* values: < 0.05: *; < 0.01: **; < 0.001: ***. Results are calculated from 3 biological replicates and reported as RQ mean ± SEM.

Table 4
The impact of schisandrin lignans on the expression of lipid and GSH metabolism genes.

Gene	Treatment	RQ value / infected	RQ value/ noninfected
PPARγ	Schisandrin	1.2 ± 0.3	1.5 ± 0.5
	Schisandrin B	6.5 ± 0.3** (*p*=0.001)	4.7 ± 0.8** (*p*=0.008)
	Schisandrin C	2.0 ± 0.5	2.3 ± 0.5
CD36	Schisandrin	0.8 ± 0.04	0.9 ± 0.2
	Schisandrin B	2.2 ± 0.3	1.6 ± 0.3
	Schisandrin C	2.0 ± 0.6	1.7 ± 0.5
ABCA1	Schisandrin	0.3 ± 0.05* (*p*=0.043)	0.4 ± 0.2
	Schisandrin B	10.1 ± 3.4** (*p*=0.005)	15.2 ± 0.1** (*p*=0.003)
	Schisandrin C	5.3 ± 1.9* (*p*=0.041)	4.0 ± 1.1
ACAT1	Schisandrin	1.7 ± 1.1	3.0 ± 0.5
	Schisandrin B	4.4 ± 1.5	8.6 ± 6.0
	Schisandrin C	1.7 ± 0.3	1.9 ± 0.3
GCLc	Schisandrin	1.4 ± 0.05	1.2 ± 0.6
	Schisandrin B	2.5 ± 0.3** (*p*=0.003)	2.2 ± 0.1* (*p*=0.018)
	Schisandrin C	1.2 ± 0.2	1.5 ± 0.3
GCLm	Schisandrin	1.6 ± 0.2	1.5 ± 0.2
	Schisandrin B	3.8 ± 0.4*** (*p*=0.0002)	2.6 ± 0.2** (*p*=0.003)
	Schisandrin C	1.8 ± 0.4* (*p*=0.0039)	1.9 ± 0.3* (*p*=0.025)
GGT1	Schisandrin	1.2 ± 0.2	2.1 ± 0.9
	Schisandrin B	4.4 ± 1.2** (*p*=0.004)	4.5 ± 0.7* (*p*=0.012)
	Schisandrin C	1.4 ± 0.4	1.2 ± 0.3

The amplification of each gene was compared to an internal reference gene GAPDH and the results were obtained by using the 2^-ΔΔCt analysis. Fold changes of RQ values above 2 and below 0.5 are considered as significant and presented as bold. Statistical significances were applied from ΔCt values, using one-way ANOVA and Dunnet's T post hoc test and they are presented as marks of *p* values: < 0.05: *; < 0.01: **; < 0.001: ***. Results are calculated from 3 biological replicates and reported as RQ mean ± SEM.

oxidation of LDL [37,38] and by this way stimulates the cholesterol and fatty acid uptake and intracellular accumulation. Consistent with earlier studies, this is seen as the appearance of lipid droplets into the *C. pneumoniae* -infected macrophages upon their exposure to native LDL, in contrast to noninfected cells treated with the same LDL preparation (Fig. 2). Out of the three studied lignans, schisandrin B and schisandrin C treatments significantly prevent the lipid loading of the macrophages, implying that they protect the cells from the infection-induced pathological changes.

Fruits from *Schisandra chinensis* are known for their wide use in oriental medicine [50]. Dibenzocyclooctadiene lignans, the main secondary metabolites in *S. chinensis* berries, have been reported to carry several biological and pharmacological activities, such as protective effects of different organ systems against chemical- and hypoxia-induced injury [51,52] and anti-cancer properties [53]. Various studies have also reported the influence of the lignans on several pathological phenomena occurring in cardiovascular diseases, such as fibrosis, inflammation and apoptosis [54]. Schisandrin B is the most widely studied among the isolated *S. chinensis* lignans, and the safety and pharmacokinetics of this lignan has been previously addressed. Single dose of orally administrated schisandrin and schisandrin B yield micromolar plasma concentrations [55,56]. High schisandrin B concentrations have also been reported to have hepatotoxic effects [57], but consistent with our data, 48 h with 50 µM concentration did not reduce the viability statistically significantly.

While there are very few studies about the antibacterial activities of schisandrin lignans, our previous findings demonstrate that *S. chinensis* extract [58] and the dibenzocyclooctadiene lignans [43] have antichlamydial activity. However, suppressing bacterial replication or affecting the infection phenotype are not likely involved in the protection of RAW264.7 macrophages from foam cell formation. According to our studies, the *C. pneumoniae* isolate CV6 does not exhibit a productive infection in RAW264.7 macrophages (data not shown). Furthermore, lipid accumulation by oxLDL uptake reduces the *C. pneumoniae* growth in macrophages [59]. In addition, earlier work demonstrates that even heat-inactivated *C. pneumoniae* is able to induce foam cell formation [36], which indicates that *Chlamydia* LPS and other structural components, rather than bacterial replication, trigger the cellular changes resulting in lipid accumulation.

Anti-inflammatory and anti-oxidative functions are generally considered to underlie the histoprotective properties of the schisandrin lignans. *S. chinensis* fruit extract decreases the NF-κB expression which regulates inflammatory cytokine expression in murine and human cell lines [60,61]. Similar results on the inhibition of NF-κB and cytokine expression in mice have been obtained with schisandrin B [62]. Furthermore, schisandrin B has been reported to affect PPARγ signaling in murine microglia, which is also involved in inflammatory response [63]. Our previous findings in human dendritic cells and THP-1 monocytes also show that schisandrin lignans suppress the inflammatory response induced by LPS of *E. coli* as well as *C. pneumoniae* infection [64].

Consistent with the earlier findings in murine microglia [63], schisandrin B upregulated the *PPARγ* expression in RAW264.7 macrophages and a similar effect was observed also with the structurally related lignan schisandrin C (Table 4). The potential relevance of *PPARγ* upregulation in the lignan-induced protection of the macrophages from foam cell formation is supported by the demonstration of this effect also in *C. pneumoniae* -infected cells. Furthermore, when RAW264.7 cells were incubated with excess LDL during *C. pneumoniae* infection, *PPARγ*, was significantly downregulated (Table 3). Downregulation of both mRNA and protein levels of PPARγ has also previously been connected to *C. pneumoniae* -induced foam cell formation [40,65].

Cellular oxidative homeostasis is one of the key regulators of lipid accumulation and antioxidative glutathione system is strongly associated with it. While the oxidative state of extracellular space has an obvious role in the degree to which LDL is modified, intracellular ROS have a central role in the signaling pathways induced by the recognition and internalization of oxLDL by macrophages [66].

The intracellular redox balance thus affects the response of macrophages to LDL, and in particular, cellular glutathione content has been related to the degree of LDL oxidation [67,68]. When cellular GSH levels are low, the LDL oxidation is accelerated which promotes foam cell formation. GSH depletion is also reported to induce LDL mediated cell injury, occurring within macrophage foam cells [69]. According to our data, schisandrin B and C elevate the total cellular glutathione levels (Fig. 3) and thereby increase the antioxidative status of the cells which may have a significant role in their ability to suppress foam cell formation (Fig. 2).

In several earlier studies, *S. chinensis* berry extract and the schisandrin lignans are reported to affect cellular glutathione metabolism in different cell types and organ systems [70–74]. For example, the fruit extract alters the expression of genes involved in GSH metabolism, such as GGT1 and glutathione S-transferase, in cardiomyocytes [75]. Schisandrin B has been reported to elevate the GSH levels e.g. in mice brain tissue [76], hepatocytes [77] and human fibroblasts [78]. In particular, studies on hepatocytes and liver tissue indicate that the enhancement of cellular GSH status by schisandrin and schisandrin B occurs by the elevation in mitochondrial GSH pools [54,79,80].

In this study, gene expression analysis on glutathione biosynthetic genes was conducted to shed light on the mechanisms by which schisandrin B and C promote the GSH levels in RAW264.7 macrophages. Our results show that schisandrin B induces the expression of both, catalytic and modifier subunits (*GCLc* and *GCLm*) of the rate limiting enzyme in glutathione biosynthesis (Table 4), which may contribute to the observed increase in cellular glutathione content (Fig. 3). Schisandrin B also induced the *GGT1* expression (Table 4), which implies to induce GGT1 activity in the plasma membrane. By breaking down the extracellular GSH and its conjugates, GGT1 activity enables the uptake of GSH precursor molecules. Our findings are in line with earlier reports with data from hepatocytes and cardiomyocytes reporting that schisandrin B increased the glutathione biosynthesis and regeneration capacity but also increased the cysteine concentration in the cells [81].

In spite of its obvious ability to elevate cellular GSH pools, schisandrin C had only a moderate effect on *GCLm* expression and no effect on *GCLc* or *GGT1* expression. This observation proposes that there are different mechanisms between schisandrin B and schisandrin C concerning their effects on GSH metabolism and highlights the central role of the modifier subunit in determining GCL enzymatic activity.

Regarding the genes related to cholesterol metabolism, our gene expression data also reveals that both schisandrin B and schisandrin C upregulated the expression of *ABCA1*, the cholesterol efflux protein (Table 4). This may result from the upregulation of PPARγ by the two lignans, since activation of PPARγ is known to promote the ABCA1 mediated cholesterol efflux [19,20]. In the case of schisandrin B, a moderate decrease in total intracellular cholesterol levels was observed (Fig. 4). Schisandrin, on the other hand, downregulated the *ABCA1* expression (Table 4). Based on the oil red O staining, schisandrin treatment did not cause alterations in macrophage lipid loading (Fig. 2) and neither did the *ABCA1* downregulation translates into quantitative differences in the macrophage cholesterol content (Fig. 4).

To study the role of cholesterol esterification in the *C. pneumoniae* -induced foam cell formation, also the expression of *ACAT1* was studied. Consistent with PPARγ downregulation, *C. pneumoniae* infection decreased the *ACAT1* expression in the presence of LDL (Table 3). This contrasts an earlier report in this respect [82] and the opposite results can be speculated to arise from the use of a cardiovascular *C. pneumoniae* isolate instead of a reference strain and a lower, physiologically more relevant LDL concentration in our study. Regarding the impact of the lignans on ACAT1 expression, increased mRNA levels were observed upon the treatment of all three derivatives (Table 4). However, cholesterol ester levels were decreased rather than elevated in the lignan-treated samples (Fig. 4), demonstrating that the cholesterol esterification in macrophages is governed by mechanisms that are much more complex than sole ACAT1 expression. In fact, even though cholesterol esterification via ACAT1 is known to have a role in macrophage foam cell formation, ACAT1 depletion has proatherogenic actions [83]. Decrease in *ACAT1* levels leads to offset in lipid balance and alteration in *ABCA1* levels. This in turn is suggested to affect cholesterol trafficking, since in mice *ACAT1* deficiency increased the intracellular lipid vacuoles which were not available for efflux. In the light of these findings, the previously proposed role of ACAT1 in *C. pneumoniae* induced foam cell formation does not seem justified.

Taken together, the protective effect of schisandrin B and schisandrin C on infection-induced foam cell formation was associated with their ability to improve the glutathione biosynthetic capacity and cholesterol trafficking of the macrophages. Upregulation of *PPARγ* along with its downstream transcriptional effects seem plausible mechanisms for mediating these effects. Besides its role in lipid metabolism, PPARγ regulates also inflammatory pathways and the redox balance of macrophages. The upregulation of *PPARγ* by schisandrin B and schisandrin C may thus contribute also to the increase in cellular glutathione content.

It has to be noted, however, that additional and alternative pathways to the PPARγ mediated induction of GSH biosynthetic enzyme upregulation may take place as a response to schisandrin lignan treatment. Another possible mechanism by which schisandrin lignans affect the glutathione metabolism of the cells, is through nuclear factor erythroid 2–related factor 2 (Nrf2) signaling. Schisandrin B has been reported to activate the Nrf2 nuclear translocation and the expression of its downstream genes [84,85]. Future studies on the interplay of PPARγ, Nrf2 and additional pathways on the biological activities of schisandrin B and schisandrin C are of great interest to deconvolute the details of the differential properties of these natural products.

Conclusions

The current work demonstrates that dibenzocyclooctadiene lignans, schisandrin B and schisandrin C decrease the foam cell formation in RAW264.7 macrophages and thus could inhibit the onset of atherosclerosis. The protective effects of schisandrin B and schisandrin C were associated with changes in macrophage glutathione metabolism, seen in both mRNA levels of key regulatory genes as well as in biochemical

quantification of the target biomolecules. The probable mechanism by which these lignans decrease the lipid accumulation in macrophages is PPARγ-mediated elevation in glutathione biosynthetic capacity in the cells and subsequently reduced lipid oxidation.

Declaration of Competing Interest

The authors declare that they have no known competing financial interests or personal relationships that could have appeared to influence the work reported in this paper.

Acknowledgment

We would like to acknowledge Petra Prebanda for excellent technical assistance. This work has been supported by the Academy of Finland grant 333291 to LH and Finnish Cultural Foundation personal grant to ET.

References

[1] G.A. Roth, C. Johnson, A. Abajobir, F. Abd-Allah, S.F. Abera, G. Abyu, M. Ahmed, B. Aksut, T. Alam, K. Alam, Global, regional, and national burden of cardiovascular diseases for 10 causes, 1990 to 2015, J. Am. Coll. Cardiol. 70 (2017) 1–25.
[2] A. Gisterå, G.K. Hansson, The immunology of atherosclerosis, Nat. Rev. Nephrol. 13 (2017) 368.
[3] J. Frostegård, Immunity, atherosclerosis and cardiovascular disease, BMC Med. 11 (2013) 117.
[4] X. Yu, Y. Fu, D. Zhang, K. Yin, C. Tang, Foam cells in atherosclerosis, Clin. Chim. Acta 424 (2013) 245–252.
[5] D.A. Chistiakov, A.A. Melnichenko, V.A. Myasoedova, A.V. Grechko, A.N. Orekhov, Mechanisms of foam cell formation in atherosclerosis, J. Mol. Med. 95 (2017) 1153–1165.
[6] A.J. Kattoor, N.V.K. Pothineni, D. Palagiri, J.L. Mehta, Oxidative stress in atherosclerosis, Curr. Atheroscler. Rep. 19 (2017) 42.
[7] X. Yang, H. Yao, Y. Chen, L. Sun, Y. Li, X. Ma, S. Duan, X. Li, R. Xiang, J. Han, Inhibition of glutathione production induces macrophage CD36 expression and enhances cellular-oxidized low density lipoprotein (oxLDL) uptake, J. Biol. Chem. 290 (2015) 21788–21799.
[8] A. Callegari, Y. Liu, C.C. White, A. Chait, P. Gough, E.W. Raines, D. Cox, T.J. Kavanagh, M.E. Rosenfeld, Gain and loss of function for glutathione synthesis: impact on advanced atherosclerosis in apolipoprotein e–deficient mice, Arterioscler. Thromb. Vasc. Biol. 31 (2011) 2473–2482.
[9] G. Gloire, S. Legrand-Poels, Piette, J. NF-κB activation by reactive oxygen species: fifteen years later, Biochem. Pharmacol. 72 (2006) 1493–1505.
[10] S.C. Lu, Glutathione synthesis, Biochim. Biophys. Acta 1830 (2013) 3143–3153.
[11] A.K. Bachhawat, A. Thakur, J. Kaur, M. Zulkifli, Glutathione transporters, Biochim. Biophys. Acta 1830 (5) (2013) 3154–3164.
[12] S.O. Rahaman, D.J. Lennon, M. Febbraio, E.A. Podrez, S.L. Hazen, R.L. Silverstein, A CD36-dependent signaling cascade is necessary for macrophage foam cell formation, Cell Metab. 4 (2006) 211–221.
[13] S. Yao, H. Tian, C. Miao, D. Zhang, L. Zhao, Y. Li, N. Yang, P. Jiao, H. Sang, S. Guo, D4F alleviates macrophage-derived foam cell apoptosis by inhibiting CD36 expression and ER stress-CHOP pathway, J. Lipid Res. 56 (2015) 836–847.
[14] M. Lee-Rueckert, R. Vikstedt, J. Metso, C. Ehnholm, P.T. Kovanen, M. Jauhiainen, Absence of endogenous phospholipid transfer protein impairs ABCA1-dependent efflux of cholesterol from macrophage foam cells, J. Lipid Res. 47 (2006) 1725–1732.
[15] S.J. Frambach, R. de Haas, J.A. Smeitink, G.A. Rongen, F.G. Russel, T.J. Schirris, Brothers in arms: ABCA1-and ABCG1-mediated cholesterol efflux as promising targets in cardiovascular disease treatment, Pharmacol. Rev. 72 (2020) 152–190 2020.
[16] D.A. Chistiakov, Y.V. Bobryshev, A.N. Orekhov, Macrophage-mediated cholesterol handling in atherosclerosis, J. Cell. Mol. Med. 20 (2016) 17–28.
[17] Y. Li, J.B. Yang, C. Jia, G.Y. Yu, Z. Pei, L. Lei, Z.Z. Wang, C.C. Chang, X.Y. Yang, T.Y. Chang, Enhancement of human ACAT1 gene expression to promote the macrophage-derived foam cell formation by dexamethasone, Cell Res. 14 (2004) 315–323.
[18] L. Maréchal, M. Laviolette, A. Rodrigue-Way, B. Sow, M. Brochu, V. Caron, A. Tremblay, The CD36-PPARγ pathway in metabolic disorders, Int. J. Mol. Sci. 19 (2018) 1529.
[19] M. Ogata, M. Tsujita, M.A. Hossain, N. Akita, F.J. Gonzalez, B. Staels, S. Suzuki, T. Fukutomi, G. Kimura, S. Yokoyama, On the mechanism for PPAR agonists to enhance ABCA1 gene expression, Atherosclerosis 205 (2009) 413–419.
[20] G. Chinetti, S. Lestavel, V. Bocher, A.T. Remaley, B. Neve, I.P. Torra, E. Teissier, A. Minnich, M. Jaye, N. Duverger, PPAR-α and PPAR-γ activators induce cholesterol removal from human macrophage foam cells through stimulation of the ABCA1 pathway, Nat. Med. 7 (2001) 53–58.
[21] G. Tumurkhuu, J. Dagvadorj, R.A. Porritt, T.R. Crother, K. Shimada, E.J. Tarling, E. Erbay, M. Arditi, S. Chen, *Chlamydia pneumoniae* hijacks a host autoregulatory IL-1β loop to drive foam cell formation and accelerate atherosclerosis, Cell Metab. 28 (2018) 432–448 e4.
[22] F.R. Stassen, T. Vainas, C.A. Bruggeman, Infection and atherosclerosis. An alternative view on an outdated hypothesis, Pharmacol. Rep. 60 (2008) 85.
[23] J.T. Grayston, Background and current knowledge of *Chlamydia pneumoniae* and atherosclerosis, J. Infect. Dis. 181 (Suppl 3) (2008) 402.
[24] C.C. Kuo, L.A. Jackson, L.A. Campbell, J.T. Grayston, *Chlamydia pneumoniae* (TWAR), Clin. Microbiol. Rev. 8 (1995) 451–461.
[25] K. Beagley, W.M. Huston, P.M. Hansbro, P. Timms, Chlamydial infection of immune cells: altered function and implications for disease, Crit. Rev. Immunol. 29 (2009) 275–305.
[26] T.C. Moazed, C. Kuo, J.T. Grayston, L.A. Campbell, Evidence of systemic dissemination of *Chlamydia pneumoniae* via macrophages in the mouse, J. Infect. Dis. 177 (1998) 1322–1325.
[27] J.A. Ramirez, Isolation of *Chlamydia pneumoniae* from the coronary artery of a patient with coronary atherosclerosis, Ann. Intern. Med. 125 (1996) 979–982.
[28] B.J. Balin, H.C. Gérard, E.J. Arking, D.M. Appelt, P.J. Branigan, J.T. Abrams, J.A. Whittum-Hudson, A.P. Hudson, Identification and localization of *Chlamydia pneumoniae* in the Alzheimer's brain, Med. Microbiol. Immunol. 187 (1998) 23–42.
[29] C.J. Hammond, L.R. Hallock, R.J. Howanski, D.M. Appelt, C.S. Little, B.J. Balin, Immunohistological detection of *Chlamydia pneumoniae* in the Alzheimer's disease brain, BMC Neurosci. 11 (2010) 121.
[30] M. Edvinsson, J. Tallkvist, C. Nyström-Rosander, N. Ilbäck, Cholesterol uptake in the mouse aorta increases during *Chlamydia pneumoniae* infection, Pathog. Dis. 75 (1) (2017) ftx004.
[31] I. Lantos, V. Endrész, D.P. Virok, A. Szabó, X. Lu, T. Mosolygó, K. Burián, *Chlamydia pneumoniae* infection exacerbates atherosclerosis in ApoB100only/LDLR−/− mouse strain, Biomed Res. Int. 2018 (2018) ID8325915.
[32] I.W. Fong, Antibiotics effects in a rabbit model of *Chlamydia pneumoniae*-induced atherosclerosis, J. Infect. Dis. 181 (Suppl 3) (2000) 514.
[33] E. Taavitsainen, M. Kortesoja, T. Bruun, N.G. Johansson, L. Hanski, Assaying *Chlamydia pneumoniae* persistence in monocyte-derived macrophages identifies dibenzocyclooctadiene lignans as phenotypic switchers, Molecules 25 (2020) 294.
[34] C.A. Gaydos, J.T. Summersgill, N.N. Sahney, J.A. Ramirez, T.C. Quinn, Replication of *Chlamydia pneumoniae* in vitro in human macrophages, endothelial cells, and aortic artery smooth muscle cells, Infect. Immun. 64 (1996) 1614–1620.
[35] S. Haranaga, H. Yamaguchi, H. Ikejima, H. Friedman, Y. Yamamoto, *Chlamydia pneumoniae* infection of alveolar macrophages: a model, J. Infect. Dis. 187 (2003) 1107–1115.
[36] M.V. Kalayoglu, G.I. Byrne, A *Chlamydia pneumoniae* component that induces macrophage foam cell formation is chlamydial lipopolysaccharide, Infect. Immun. 66 (1998) 5067–5072.
[37] R. Dittrich, C. Dragonas, A. Mueller, T. Maltaris, J. Rupp, M.W. Beckmann, M. Maass, Endothelial *Chlamydia pneumoniae* infection promotes oxidation of LDL, Biochem. Biophys. Res. Commun. 319 (2004) 501–505.
[38] M.V. Kalayoglu, B. Hoerneman, D. LaVerda, S.G. Morrison, R.P. Morrison, G.I. Byrne, Cellular oxidation of low-density lipoprotein by *Chlamydia pneumoniae*, J. Infect. Dis. 180 (1999) 780–790.
[39] W. Liu, P. He, B. Cheng, C. Mei, Y. Wang, J. Wan, *Chlamydia pneumoniae* disturbs cholesterol homeostasis in human THP-1 macrophages via JNK-PPARγ dependent signal transduction pathways, Microb. Infect. 12 (2010) 1226–1235.
[40] B. Cheng, X. Wu, S. Sun, Q. Wu, C. Mei, Q. Xu, J. Wu, P. He, MAPK–PPARα/γ signal transduction pathways are involved in *Chlamydia pneumoniae*-induced macrophage-derived foam cell formation, Microb. Pathog. 69 (2014) 1–8.
[41] T. Kitazawa, A. Fukushima, S. Okugawa, S. Yanagimoto, K. Tsukada, K. Tatsuno, K. Koike, S. Kimura, T. Kishimoto, Y. Shibasaki, Chlamydophilal antigens induce foam cell formation via c-jun NH2-terminal kinase, Microb. Infect. 9 (2007) 1410–1414.
[42] W. Liu, P. He, B. Cheng, C. Mei, Y. Wang, J. Wan, *Chlamydia pneumoniae* disturbs cholesterol homeostasis in human THP-1 macrophages via JNK-PPARγ dependent signal transduction pathways, Microb. Infect. 12 (2010) 1226–1235.
[43] E. Hakala, L. Hanski, H. Uvell, T. Yrjönen, H. Vuorela, M. Elofsson, P.M. Vuorela, Dibenzocyclooctadiene lignans from *Schisandra spp.* selectively inhibit the growth of the intracellular bacteria *Chlamydia pneumoniae* and *Chlamydia trachomatis*, J. Antibiot. 68 (2015) 609–614.
[44] M. Maass, C. Bartels, P.M. Engel, U. Mamat, H. Sievers, Endovascular presence of viable *Chlamydia pneumoniae* is a common phenomenon in coronary artery disease, J. Am. Coll. Cardiol. 31 (1998) 827–832.
[45] C.C. Kuo, J.T. Grayston, A sensitive cell line, HL cells, for isolation and propagation of *Chlamydia pneumoniae* strain TWAR, J. Infect. Dis. 162 (1990) 755–758.
[46] M. Kortesoja, R.E. Trofin, L. Hanski, A platform for studying the transfer of *Chlamydia pneumoniae* infection between respiratory epithelium and phagocytes, J. Microbiol. Methods 171 (2020) 105857.
[47] I. Rahman, A. Kode, S.K. Biswas, Assay for quantitative determination of glutathione and glutathione disulfide levels using enzymatic recycling method, Nat. Protoc. 1 (2006) 3159.
[48] F. Cao, A. Castrillo, P. Tontonoz, F. Re, G.I. Byrne, *Chlamydia pneumoniae*-induced macrophage foam cell formation is mediated by toll-like receptor 2, Infect. Immun. 75 (2007) 753–759.
[49] L.A. Campbell, M. Rosenfeld, C. Kuo, The role of *Chlamydia pneumoniae* in atherosclerosis–recent evidence from animal models, Trends Microbiol. 8 (2000) 255–257.
[50] A. Szopa, R. Ekiert, H. Ekiert, Current knowledge of *Schisandra chinensis* (Turcz.) Baill. (Chinese magnolia vine) as a medicinal plant species: a review on the bioactive components, pharmacological properties, analytical and biotechnological studies, Phytochem. Rev. 16 (2017) 195–218.
[51] P.Y. Chiu, M.H. Tang, D.H. Mak, M.K. Poon, K.M. Ko, Hepatoprotective mechanism of schisandrin B: role of mitochondrial glutathione antioxidant status and heat shock proteins, Free Radic. Biol. Med. 35 (2003) 368–380.

[52] T.H. Lee, C.H. Jung, D. Lee, Neuroprotective effects of schisandrin B against transient focal cerebral ischemia in Sprague–Dawley rats, Food Chem. Toxicol. 50 (2012) 4239–4245.
[53] Z. Liu, B. Zhang, K. Liu, Z. Ding, X. Hu, Schisandrin B attenuates cancer invasion and metastasis via inhibiting epithelial-mesenchymal transition, PLoS ONE 7 (2012) e40480.
[54] J.N. Chun, M. Cho, I. So, J. Jeon, The protective effects of *Schisandra chinensis* fruit extract and its lignans against cardiovascular disease: a review of the molecular mechanisms, Fitoterapia 97 (2014) 224–233.
[55] Z. Wang, L. You, Y. Cheng, K. Hu, Z. Wang, Y. Cheng, J. Yang, Y. Yang, G. Wang, Investigation of pharmacokinetics, tissue distribution and excretion of schisandrin B in rats by HPLC–MS/MS, Biomed. Chromatogr. 32 (2018) e4069.
[56] C. Li, Y. Cheng, C. Hsieh, T. Tsai, Pharmacokinetics of schizandrin and its pharmaceutical products assessed using a validated LC–MS/MS method, Molecules 23 (2018) 173.
[57] ... Y. Zhang, Z.W. Zhou, H. Jin, C. Hu, Z.X. He, Z.L. Yu, S.F. Zhou, Schisandrin B inhibits cell growth and induces cellular apoptosis and autophagy in mouse hepatocytes and macrophages: implications for its hepatotoxicity, Drug Des. Dev. Ther 9 (2015) 2001.
[58] E. Hakala, L.L. Hanski, T. Yrjönen, H.J. Vuorela, P.M. Vuorela, The lignan-containing extract of *Schisandra chinensis* berries inhibits the growth of *Chlamydia pneumoniae*, Nat. Prod. Commun. 10 (2015) 1001–1004.
[59] E. Blessing, C. Kuo, T. Lin, L.A. Campbell, F. Bea, B. Chesebro, M.E. Rosenfeld, Foam cell formation inhibits growth of *Chlamydia pneumoniae* but does not attenuate *Chlamydia pneumoniae*–induced secretion of proinflammatory cytokines, Circulation 105 (2002) 1976–1982.
[60] Y.S. Kang, M.H. Han, S.H. Hong, C. Park, H.J. Hwang, B.W. Kim, K.H. Kyoung, Y.W. Choi, C.M. Kim, Y.H. Choi, Anti-inflammatory effects of *Schisandra chinensis* (turcz.) baill fruit through the inactivation of nuclear factor-kappaB and mitogen-activated protein kinases signaling pathways in lipopolysaccharide-stimulated murine macrophages, J. Cancer Prev. 19 (2014) 279–287.
[61] O.H. Kang, H. Chae, J. Choi, H.J. Choi, P.S. Park, S.H. Cho, G. Lee, H. So, Y.K. Choo, O. Kweon, Effects of the *Schisandra* fructus water extract on cytokine release from a human mast cell line, J. Med. Food 9 (2006) 480–486.
[62] P. Chen, S. Pang, N. Yang, H. Meng, J. Liu, N. Zhou, M. Zhang, Z. Xu, W. Gao, B. Chen, Beneficial effects of schisandrin B on the cardiac function in mice model of myocardial infarction, PLoS ONE 8 (11) (2013) e79418.
[63] N. Liu, J. Zheng, Y. Zhuang, Z. Zhou, J. Zhao, L. Yang, Anti-inflammatory effects of schisandrin B on LPS-stimulated BV2 microglia via activating PPAR-γ, Inflammation 40 (2017) 1006–1011.
[64] M. Kortesoja, E. Karhu, E.S. Olafsdottir, J. Freysdottir, L. Hanski, Impact of dibenzocyclooctadiene lignans from *Schisandra chinensis* on the redox status and activation of human innate immune system cells, Free Radic. Biol. Med. 131 (2019) 309–317.
[65] C. Mei, P. He, B. Cheng, W. Liu, Y. Wang, J. Wan, *Chlamydia pneumoniae* induces macrophage-derived foam cell formation via PPAR α and PPAR γ-dependent pathways, Cell Biol. Int. 33 (2019) 301–308.
[66] I. Levitan, S. Volkov, P.V. Subbaiah, Oxidized LDL: diversity, patterns of recognition, and pathophysiology, Antioxid. Redox Signal. 13 (2010) 39–75.
[67] M. Rosenblat, R. Coleman, M. Aviram, Increased macrophage glutathione content reduces cell-mediated oxidation of LDL and atherosclerosis in apolipoprotein E-deficient mice, Atherosclerosis 163 (2002) 17–28.
[68] M. Aviram, B. Fuhrman, LDL oxidation by arterial wall macrophages depends on the oxidative status in the lipoprotein and in the cells: role of prooxidants vs. antioxidants, in: Anonymous *Molecular and Cellular Effects of Nutrition on Disease Processes*, Springer, 1998, pp. 149–159.
[69] Y. Wang, M. Qiao, J.J. Mieyal, L.M. Asmis, R. Asmis, Molecular mechanism of glutathione-mediated protection from oxidized low-density lipoprotein-induced cell injury in human macrophages: role of glutathione reductase and glutaredoxin, Free Radic. Biol. Med. 41 (2006) 775–785.
[70] P.K. Leong, H.S. Wong, J. Chen, W.M. Chan, H.Y. Leung, K.M. Ko, Differential action between schisandrin A and schisandrin B in eliciting an anti-inflammatory action: the depletion of reduced glutathione and the induction of an antioxidant response, PLoS ONE 11 (5) (2016) e0155879.
[71] P.Y. Lam, K. Ming Ko, (-)Schisandrin B ameliorates paraquat-induced oxidative stress by suppressing glutathione depletion and enhancing glutathione recovery in differentiated PC12 cells, Biofactors 37 (2011) 51–57.
[72] P.Y. Chiu, H.Y. Leung, K.M. Ko, Schisandrin B enhances renal mitochondrial antioxidant status, functional and structural integrity, and protects against gentamicin-induced nephrotoxicity in rats, Biol. Pharm. Bull. 31 (2008) 602–605.
[73] L.I. Yan-Zi, M. Zhi-Na, S. Yin-Shi, R. Shen, S. Jiang, W. Zhang, W. Zi, L.I. Wei, Protective effects of extracts of *Schisandra chinensis* stems against acetaminophen-induced hepatotoxicity via regulation of MAPK and caspase-3 signaling pathways, Chin. J. Nat. Med. 16 (2018) 700–713.
[74] J. Zhai, F. Zhang, S. Gao, L. Chen, G. Feng, J. Yin, W. Chen, *Schisandra chinensis* extract decreases chloroacetaldehyde production in rats and attenuates cyclophosphamide toxicity in liver, kidney and brain, J. Ethnopharmacol. 210 (2018) 223–231.
[75] E.H. Choi, N. Lee, H.J. Kim, M.K. Kim, S. Chi, D.Y. Kwon, H.S. Chun, *Schisandra* fructus extract ameliorates doxorubicin-induce cytotoxicity in cardiomyocytes: altered gene expression for detoxification enzymes, Genes Nutr. 2 (2008) 337–345.
[76] K. Ko, B.Y. Lam, Schisandrin B protects against tert-butylhydroperoxide induced cerebral toxicity by enhancing glutathione antioxidant status in mouse brain, Mol. Cell. Biochem. 238 (2002) 181–186.
[77] P.Y. Chiu, M.H. Tang, D.H. Mak, M.K. Poon, K.M. Ko, Hepatoprotective mechanism of schisandrin B: role of mitochondrial glutathione antioxidant status and heat shock proteins, Free Radic. Biol. Med. 35 (2003) 368–380.
[78] P.Y. Chiu, P.Y. Lam, C.W. Yan, K.M. Ko, Schisandrin B protects against solar irradiation-induced oxidative injury in BJ human fibroblasts, Fitoterapia 82 (2011) 682–691.
[79] S.P. Ip, M.K. Poon, C.T. Che, K.H. Ng, Y.C. Kong, K.M. Ko, Schisandrin B protects against carbon tetrachloride toxicity by enhancing the mitochondrial glutathione redox status in mouse liver, Free Radic. Biol. Med. 21 (1996) 709–712.
[80] S. Ip, C. Ma, C. Che, K. Ko, Methylenedioxy group as determinant of schisandrin in enhancing hepatic mitochondrial glutathione in carbon tetrachloride-intoxicated mice, Biochem. Pharmacol. 54 (1997) 317–319.
[81] P.Y. Chiu, K.M. Ko, Schisandrin B-induced increase in cellular glutathione level and protection against oxidant injury are mediated by the enhancement of glutathione synthesis and regeneration in AML12 and H9c2 cells, BioFactors 26 (2006) 221–230.
[82] P. He, C. Mei, B. Cheng, W. Liu, Y. Wang, J. Wan, *Chlamydia pneumoniae* induces macrophage-derived foam cell formation by up-regulating acyl-coenzyme A: cholesterol acyltransferase 1, Microb. Infect. 11 (2009) 157–163.
[83] D. Akopian, J.D. Medh, Macrophage ACAT depletion: mechanisms of atherogenesis, Curr. Opin. Lipidol. 17 (2006) 85.
[84] R. Checker, R.S. Patwardhan, D. Sharma, J. Menon, M. Thoh, H.N. Bhilwade, T. Konishi, S.K. Sandur, Schisandrin B exhibits anti-inflammatory activity through modulation of the redox-sensitive transcription factors Nrf2 and NF-κB, Free Radic. Biol. Med. 53 (2012) 1421–1430.
[85] P.K. Leong, P.Y. Chiu, N. Chen, H. Leung, K.M. Ko, Schisandrin B elicits a glutathione antioxidant response and protects against apoptosis via the redox-sensitive ERK/Nrf2 pathway in AML12 hepatocytes, Free Radic. Res. 45 (2011) 483–495.